

Retraction for *RSC Advances*:

---

**Broadband cavity enhanced absorption spectroscopy (BBCEAS) as a detection technique for a microfluidic flow cell made of Zeonor®**

Ruchi Gupta, N J Goddard, Stephan Mohr, Cathy M. Rushworth, Claire Vallance and Yathukulan Yogarajah

*RSC Adv.*, 2013, DOI: 10.1039/C2RA22732K. **Retraction published 17th September 2013**

---

We, the named authors, hereby wholly retract this *RSC Advances* article due to problems with the reliability and reproducibility of some of the data quoted in the article. This article was submitted for publication without the knowledge and approval of any of the Oxford-based authors, therefore Claire Vallance, Cathy Rushworth and Yathukulan Yogarajah disassociate themselves from the content of the article.

Signed: Ruchi Gupta, N J Goddard, Stephan Mohr, Cathy M. Rushworth, Claire Vallance and Yathukulan Yogarajah, September 2013

Retraction endorsed by Sarah Ruthven, Managing Editor, *RSC Advances*

---

# RSC Advances

## Accepted Manuscript



This is an *Accepted Manuscript*, which has been through the RSC Publishing peer review process and has been accepted for publication.

*Accepted Manuscripts* are published online shortly after acceptance, which is prior to technical editing, formatting and proof reading. This free service from RSC Publishing allows authors to make their results available to the community, in citable form, before publication of the edited article. This *Accepted Manuscript* will be replaced by the edited and formatted *Advance Article* as soon as this is available.

To cite this manuscript please use its permanent Digital Object Identifier (DOI®), which is identical for all formats of publication.

More information about *Accepted Manuscripts* can be found in the [Information for Authors](#).

Please note that technical editing may introduce minor changes to the text and/or graphics contained in the manuscript submitted by the author(s) which may alter content, and that the standard [Terms & Conditions](#) and the [ethical guidelines](#) that apply to the journal are still applicable. In no event shall the RSC be held responsible for any errors or omissions in these *Accepted Manuscript* manuscripts or any consequences arising from the use of any information contained in them.

# Broadband cavity enhanced absorption spectroscopy (BBCEAS) as a detection technique for a microfluidic flow cell made of Zeonor<sup>®</sup>

## Abstract

Broadband cavity enhanced absorption spectroscopy (BBCEAS) has so far been used for increasing the effective optical path length and hence detection sensitivity of flow cells made of high-optical quality glass. Glass, however, is fragile, expensive and difficult to process. In this work, the feasibility of BBCEAS for high sensitivity detection in a microfluidic flow cell made of a cyclic olefin copolymer, Zeonor<sup>®</sup> has been demonstrated for the first time. The Zeonor<sup>®</sup> device is disposable and is suitable for applications in areas such as clinical diagnostics, where glass devices would be unsuitable. The effective number of passes of light through the Zeonor<sup>®</sup> device was increased by two orders of magnitude on placing it between two 99±0.3% reflectivity broadband (400-800 nm) mirrors. At 572 nm, the minimum detectable absorption coefficient (i.e. absorbance per unit length) achieved using the Zeonor<sup>®</sup> device was  $2.9 \times 10^{-3} \text{ cm}^{-1}$ , which corresponds to a limit of detection of 1.1  $\mu\text{M}$  potassium permanganate solution. This is two orders of magnitude better than the typical LOD achieved by performing single pass absorbance measurements in microfluidic devices.

**Keywords:** absorption spectroscopy, Zeonor<sup>®</sup>, cavity enhanced, microfluidics, sensitivity.

## 1. Introduction

Microfluidic devices offer a number of useful properties, such as high throughput, low-cost, portability, and the potential for automation and use in remote sensing or field studies [1]. Such devices present an ideal platform for point-of-care testing, clinical and forensic analysis, medical diagnostics, environmental monitoring and food analysis [2-3]. In addition, microfluidic devices are particularly beneficial for applications in which the liquid volume used must be minimised, either due to high reagent costs or limited sample availability.

On one hand the small fluid volumes involved in microfluidic devices are advantageous, but on the other hand they pose a significant challenge to high sensitivity detection in microchannels [4]. Laser induced fluorescence (LIF) is commonly used to perform high sensitivity detection in microfluidic devices [4]. However, as most compounds do not show native fluorescence, LIF detection requires extra labelling chemistries. These labelling protocols are usually lengthy and often have to be carried out off-chip. In addition, tagging of

35 analytes with fluorophores can result in incomplete derivatisation (and hence errors in  
36 quantitative results) or formation of multiple peaks due to multi-derivatisation, or both [5]. In  
37 comparison to LIF, absorption spectroscopy does not require extra labelling chemistries,  
38 since all species absorb over some wavelength range within the electromagnetic spectrum. In  
39 addition, broadband absorption spectroscopy is advantageous because the full spectral profile  
40 of a species can be obtained in a single measurement which can permit its identification. The  
41 detection sensitivity of single pass absorption spectroscopy for microfluidic devices is,  
42 however, poor because the optical path length through the sample is small. Thus, a number of  
43 approaches have been developed to increase the optical path length through the sample and  
44 hence to achieve high sensitivity absorption spectroscopy in microfluidic devices.

45

46 The distance travelled by light through the sample has, for example, been increased using  
47 liquid core waveguides (LCW) which rely on total internal reflection to confine light in liquid  
48 samples. This implies that LCWs require using either high refractive index liquids (e.g.  
49 aromatics, carbon disulphide and halogenated compounds) [6-8] or using tubes made of low  
50 refractive index polymers such as Teflon [9] or coating the walls of flow cells with Teflon  
51 [10]. The use of high refractive index liquids, however, limits the type of chemistry that may  
52 be used. The integration of Teflon tubing with microfluidic systems is cumbersome and  
53 polymer-coated flow cells have limited long-term performance as a result of degradation of  
54 the coating. Alternatively, anti-resonant reflecting optical waveguides (ARROW) have been  
55 used to perform high sensitivity detection in microfluidic flow cells. In ARROW, light is  
56 confined into a liquid sample by coating the walls of flow cells with dielectric mirrors [11-  
57 12]. ARROWs, however, are difficult to fabricate and place constraints on the dimensions of  
58 microfluidic flow cells.

59

60 The optical path length has also been increased by placing waveguides parallel to the long  
61 axis of flow cells [13] and allowing the evanescent field of light travelling in the waveguide  
62 to interact with the sample. The effectiveness of this scheme, however, requires maximising  
63 the fraction of optical mode power propagating in the evanescent region. Thus, tapered and  
64 U-bend waveguides have been used to “push” the evanescent field deeper into the sample  
65 layer [14-15]. The coupling of light into waveguides has been cumbersome because it  
66 requires alignment of the light beam with the sub-micron thickness of the waveguide [16].  
67 The distance over which the evanescent light wave interacts with the sample has also been  
68 enhanced using whispering gallery mode (WGM) microresonators [17-18]. Some limitations

69 of WGM microresonators are as follows: Firstly, such structures can in general only be used  
70 to record absorbance over a relatively narrow range of wavelengths which is governed by the  
71 availability of tuneable lasers. Secondly, microresonators are point detectors and hence need  
72 to be fabricated at desired locations to monitor absorbance at different points in microfluidic  
73 flow cells. Finally, the fabrication methods (e.g. high power lasers and oxy-hydrogen flames)  
74 currently used to make WGM microspheres require a degree of skill and are not suitable for  
75 mass production. In contrast, broadband cavity enhanced absorption spectroscopy (BBCEAS)  
76 offers a relatively simple approach to increasing the optical path length by several orders of  
77 magnitude by placing a microfluidic device within an optical cavity comprising two high  
78 reflectivity mirrors.

79

80 To our knowledge, BBCEAS has so far only been used as a detection technique for flow cells  
81 made of glass [19-20]. This is because glass has high optical transmission in the visible  
82 region of the electromagnetic spectrum, and can be manufactured with high surface quality.  
83 This in turn minimises scattering and absorption losses introduced by a glass flow cell placed  
84 in an optical cavity made of high reflectivity mirrors. As a result, the total number of  
85 effective passes of light (and hence the optical path length) through the sample is increased.  
86 Glass is, however, expensive and fragile relative to other materials in widespread use in  
87 microfluidics. In addition, the fabrication of glass-based devices often requires the use of  
88 harmful chemicals such as hydrofluoric acid, and sealing the devices by thermal bonding is a  
89 slow process which can have a high failure rate [21-22]. It is also difficult to drill fluidic  
90 connection ports in devices made of glass. In contrast to glass, Zeonor<sup>®</sup>-based flow cells can  
91 be made using a number of fabrication techniques (e.g. injection moulding) that are suitable  
92 for mass production of devices [23-24]. In addition, Zeonor<sup>®</sup> costs at least 10 times less than  
93 glass. As a result, the use of cyclic olefin copolymers such as Zeonor<sup>®</sup> is gaining popularity  
94 for constructing low cost disposable microfluidic devices [25]. This work, for the first time,  
95 investigates the feasibility of BBCEAS as a detection technique for a microfluidic device  
96 made of Zeonor<sup>®</sup> fabricated using pressure sensitive adhesive bonding. Limit of detection  
97 (LOD) and the effective number of passes of light for the device has been estimated using  
98 dilute samples of potassium permanganate.

99

## 100 **2. Experimental**

### 101 *2.1 Chemicals*

102 Potassium permanganate used in this work was purchased from Sigma-Aldrich ( $\geq 99\%$ ,  
103 Sigma-Aldrich, Gillingham, UK). All solutions were made up using 18.2 M $\Omega$  water (Elix<sup>®</sup>,  
104 Millipore, UK).

105

## 106 2.2 Microfabrication

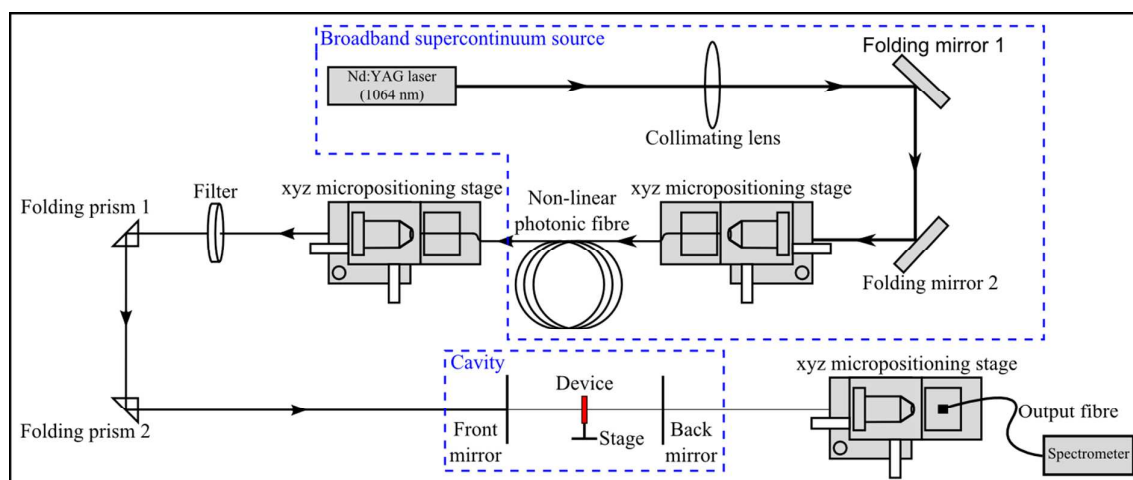
107 A commercial flow cell from Starna, Essex, UK (catalogue number: 45/Q/0.1) of path length  
108 100  $\mu\text{m}$  was used as a high-optical quality standard for comparison with the measurements  
109 employing the microfluidic device made of Zeonor<sup>®</sup> (shown in Figure S1). In order to  
110 construct the Zeonor<sup>®</sup> device, a 5 mm wide and 2.8 cm long window was cut into 80  $\mu\text{m}$  thick  
111 pressure sensitive adhesive (3M8153LE, Viking Industrial Products Ltd, Keighley, UK)  
112 using a scalpel. In addition, access holes of 1 mm diameter were drilled through 188  $\mu\text{m}$  thick  
113 Zeonor<sup>®</sup> film (ZF14-188, Zeon Corporation, Tokyo). The channel was formed by placing the  
114 pressure sensitive adhesive in between the Zeonor<sup>®</sup> film with access holes and another piece  
115 of the Zeonor<sup>®</sup> film. In order to impart mechanical rigidity to the Zeonor<sup>®</sup> device, it was  
116 clamped onto a plastic frame manufactured in-house by CNC machining. Finally, the fluidic  
117 connections for the Zeonor<sup>®</sup> device were made using in-house manufactured connectors.

118

## 119 2.3 Instrumentation

120 A schematic of the experimental set-up is shown in Figure 1.

121



122

123

124

125 Broadband supercontinuum light was generated by pumping a non-linear photonic crystal  
126 (microstructured) fibre (SC-5.0-1040, NKT Photonics, Germany) with the focussed 1064 nm

127 output of a Nd:YAG laser (NP-10620-100, Teem Photonics, Edinburgh, UK). The output  
128 from the fibre passed through an objective (06 OD 03, Comar Instruments Ltd, Cambridge,  
129 UK) and a bandpass filter (FGS900, Thorlabs, Cambridge, UK), yielding a collimated beam  
130 with a bandwidth of 480-710 nm. The light beam was steered using two right angle prisms  
131 (16 RX 01, Comar, Cambridge) into the optical cavity. The cavity was formed from two high  
132 reflectivity concave mirrors ( $R_{400-800\text{ nm}} = 99 \pm 0.3\%$  and radius of curvature = 1 m, Layertec,  
133 Germany) placed 13 cm apart. The light exiting the cavity was focussed using an objective  
134 (25 OD 09, Comar, Cambridge, UK) and coupled to a spectrometer (HR4000, 10  $\mu\text{m}$  slit,  
135 Ocean Optics, Germany) using a multimode optical fibre (M15L02, Thorlabs, Cambridge,  
136 UK) with a core diameter of 105  $\mu\text{m}$ . The spectrometer was USB interfaced to a computer  
137 and data was acquired via a LabVIEW (National Instruments, Texas, USA) program.

138

139 The flow cell was mounted onto an assembly of optical stages (M-423, M-443-4, Newport,  
140 Oxfordshire, UK and 70 XT 65, Comar, Cambridge, UK) to permit its linear movement in the  
141 directions perpendicular to the propagation axis of light and rotational movement in the  
142 horizontal and vertical planes. The device was placed at the centre of the optical cavity at  
143 normal incidence to the propagation axis of light. While reflection losses associated with the  
144 chip can in some cases be reduced by placing the device at Brewster's angle within the  
145 cavity, for high quality devices with all surfaces parallel, inserting the device at right angles  
146 to the beam path allows light reflected from the surfaces to be recycled into the cavity [26].  
147 The latter configuration was chosen both for the ease of cavity alignment and because it  
148 provides a well-defined (single pass) optical path length. The optical power incident on the  
149 device is estimated to be 300 mW because the supercontinuum source generated pulses of  
150 duration of 1 ns with an energy of 3  $\mu\text{J}$ , of which  $R_{400-800\text{ nm}}^2$  was coupled inside the cavity.

151

#### 152 *2.4 Experimental procedure*

153 In BBCEAS, light is injected continuously into an optical cavity, and the time-integrated light  
154 intensity emerging from the cavity is dispersed into its constituent wavelengths prior to  
155 detection. The wavelength-dependent absorbance,  $A$ , is defined as [22]:

156

$$157 \quad A = \varepsilon cl = \frac{(I_0 / I) - 1}{\text{CEF}} \quad (1)$$

158

159 where  $\varepsilon$  is the wavelength-dependent molar extinction coefficient,  $c$  is the sample  
160 concentration,  $l$  is the single pass optical path length through the sample,  $I_0$  and  $I$  are the  
161 measured intensity of light in the absence and the presence of the sample respectively. The  
162 absorption coefficient (is absorbance per unit length) can be calculated as a product of  
163 concentration and molar extinction coefficient. CEF is the cavity enhancement factor, which  
164 is a measure of the effective number of passes of light through the sample for a given  
165 experimental set-up. The total optical loss associated with the set-up was estimated by taking  
166 the inverse of the CEF [27].

167

168 The optical cavity was initially aligned such that all back reflections from the mirrors and  
169 surfaces within the microfluidic device were merged with the path of the incident beam. The  
170 alignment of the mirrors and microfluidic device was then fine tuned to optimise the intensity  
171 of the output signal of the cavity. Unless stated otherwise, a spectrometer integration time of  
172 10 ms was used for all the experiments.

173

174 A dilution series of potassium permanganate solutions in the concentration range from  
175  $2.5 \times 10^{-5}$  M to  $1 \times 10^{-3}$  M was prepared. Solutions were introduced into the device using a  
176 syringe pump (Fusion 400, Chemyx, Stafford, UK) fitted with a 10 ml plastic syringe (BD,  
177 Oxford, UK). For each absorption measurement, the microfluidic device was initially flushed  
178 with 1.5 ml of deionised water at a flow rate of 0.5 ml/min, and the output spectrum of the  
179 cavity over the wavelength range from 480-710 nm was recorded, averaged over 50 traces.  
180 This spectrum constituted the baseline absorption measurement ( $I_0$  in Equation (1)). The  
181 device was then flushed with the appropriate potassium permanganate solution and the  
182 spectrum recorded to obtain the 'signal' absorption measurement ( $I$  in Equation (1)). These  
183 steps were repeated 3 times for each concentration of potassium permanganate solution.

184

185 The molar extinction coefficient,  $\varepsilon$ , of potassium permanganate was determined in the  
186 wavelength range between 400 nm and 800 nm (as shown in Figure S2) using a commercial  
187 UV-vis spectrometer (Cary 100 Bio UV-Vis, Varian, Sussex, UK). The single pass optical  
188 path length,  $l$ , in Equation (1) is governed by the physical dimension of the flow cell along  
189 the path of the light beam. The data was substituted into Equation (1) to calculate the CEF for  
190 each device. The LOD was determined using a plot of measured wavelength-dependent  
191 absorbance against the concentration of potassium permanganate solutions. The LOD is given



192 by the y-axis intercept plus three times the standard deviation,  $s_B$ , associated with that value.  
193 The standard deviation,  $s_B$ , was calculated as follows [28]:

194

$$195 \quad s_B = \sqrt{\frac{\sum (y_i - \hat{y}_i)^2}{n-1} \frac{\sum x_i^2}{n \sum (x_i - \bar{x})^2}} \quad (2)$$

196

197 where  $y_i$  is the observed absorbance,  $\hat{y}_i$  is the calculated absorbance,  $n$  is the number of data  
198 points,  $x_i$  is the concentration of potassium permanganate solutions used and  $\bar{x}$  is the mean  
199 of the concentration of potassium permanganate solutions.

200

### 201 **3. Results and discussion**

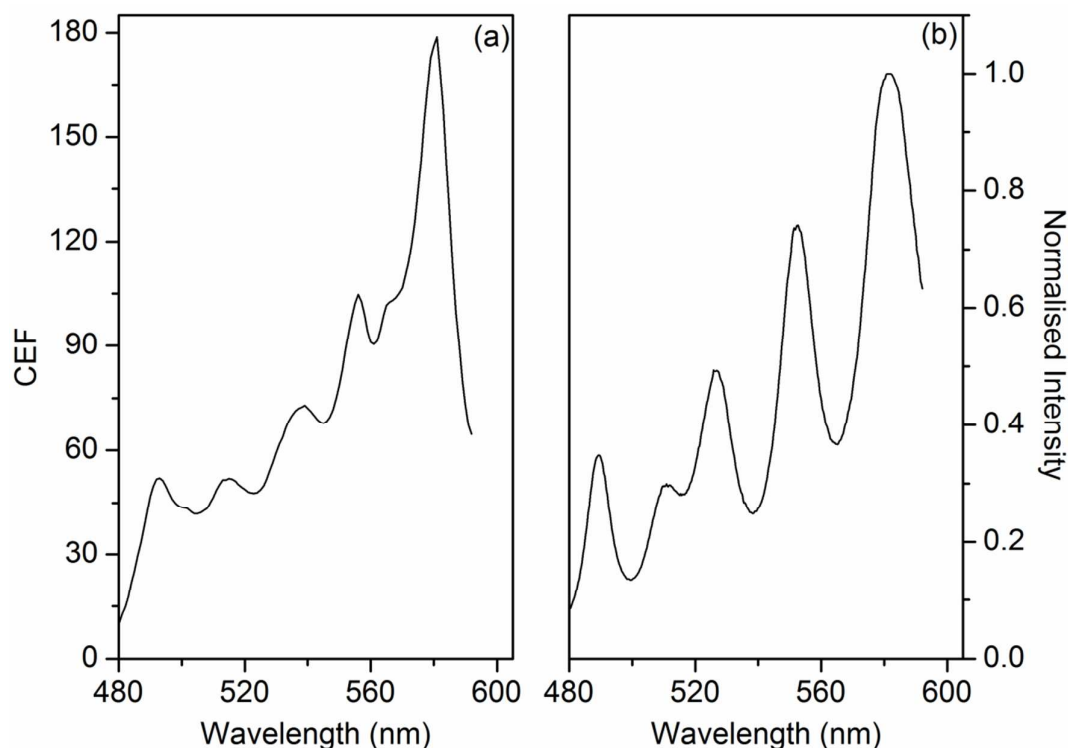
#### 202 *3.1 Initial study*

203 Light injected into the cavity had a bandwidth of 480-710 nm and potassium permanganate  
204 absorbs between 450 nm and 600 nm. The mirrors used have a reflectivity of  $99 \pm 0.3\%$  in the  
205 wavelength range from 400 nm to 800 nm. The shortest wavelength of light with 92%  
206 transmission through (Spectrosil<sup>®</sup> quartz) glass and (ZF14-188) Zeonor<sup>®</sup> is approximately  
207 190 nm and 300 nm [29] respectively. Thus, the feasibility of BBCEAS as a detection  
208 technique was studied in the wavelength range between 480 nm and 600 nm, where the lower  
209 and upper limits were determined by the supercontinuum light source and the absorbance  
210 spectrum of potassium permanganate respectively. Despite the limited wavelength range  
211 studied in this work, the detection scheme used is universal provided that appropriate light  
212 sources, mirrors and absorbing species are chosen.

213

214 A commercial flow cell made of high-optical quality glass was placed inside the cavity to  
215 determine the CEF as a function of wavelength for the reference system (see Figure 2 (a)).  
216 CEF is inversely related to the total optical loss, which is determined by the reflectivity of the  
217 mirrors comprising the optical cavity as well as by scattering and absorption characteristics of  
218 the flow cell placed inside the cavity. Based on the data provided by the manufacturer, the  
219 scattering and absorption characteristics of the glass flow cell were independent of the  
220 wavelength in the range between 480 nm and 600 nm. The reflectivity of large bandwidth  
221 mirrors used in this work, however, was variable in the wavelength range studied because  
222 they were constructed by depositing multiple dielectric layers. The variations in the  
223 reflectivity of mirrors with wavelength can be observed by considering a typical output

224 spectrum of the cavity, which is shown in Figure 2 (b). The intensity of light exiting the  
225 cavity is high at wavelengths where the reflectivity of mirrors comprising the cavity is high  
226 (and hence losses are low). This implies that the dependence of CEF on the wavelength of the  
227 excitation light is due to variations in the mirror reflectivity with wavelength. As a result, the  
228 total optical loss and hence the CEF were a function of the wavelength of the excitation light.  
229 As shown in Figure 2 (a), the maximum CEF for the glass flow cell was 178 and was  
230 obtained approximately at the wavelength where the intensity of light exiting the cavity was  
231 the highest. This corresponds to the wavelength at which the total optical loss was lowest.  
232



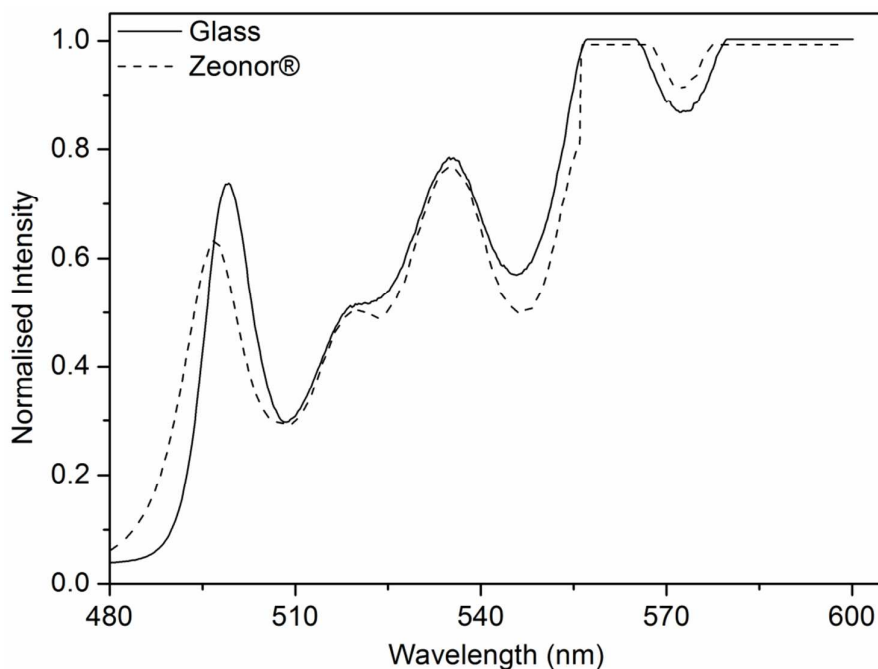
233  
234 **Figure 2: Plot of (a) CEF vs. wavelength for the commercial flow cell made of high-**  
235 **optical quality glass (spectrometer integration time is 10 ms) and (b) cavity output**  
236 **spectrum without a flow cell (spectrometer integration time is 3 ms and was chosen to**  
237 **avoid signal saturation)**

238

### 239 3.2 Investigation with the microfluidic flow cell made of Zeonor<sup>®</sup>

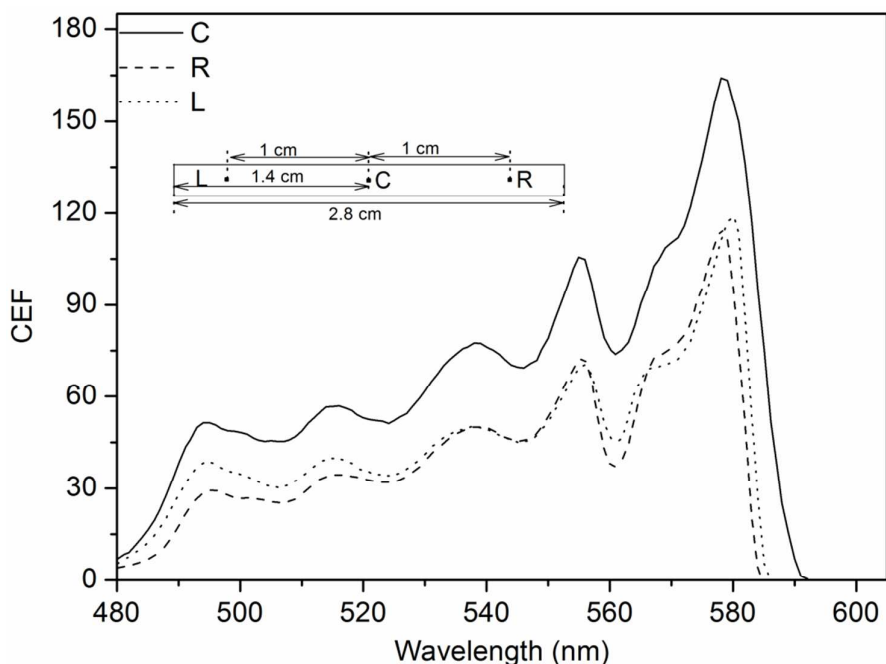
240 A comparison of the cavity output spectra of the microfluidic device made of Zeonor<sup>®</sup> and  
241 glass flow cells is shown in Figure 3. The intensity of light exiting the cavity with the  
242 Zeonor<sup>®</sup> device was similar to the glass flow cell, thereby suggesting that the optical losses  
243 associated with the two were comparable. A plot of the CEF of the Zeonor<sup>®</sup> device as a

244 function of the wavelength of the excitation light is shown in Figure 4. A comparison of  
 245 Figure 2 (a) and Figure 4 shows that the CEF of the Zeonor<sup>®</sup> device was comparable to the  
 246 glass flow cell. Subsequently, the CEF of the Zeonor<sup>®</sup> device was measured at three different  
 247 spatial locations, which are shown in the inset in Figure 4, by moving the selected regions of  
 248 the device in the path of the light beam. As shown in Figure 4, the CEF at the “L” and “R”  
 249 locations of the Zeonor<sup>®</sup> device is ~80 at 572 nm, which is ~31% lower than the CEF at “C”.  
 250 This could be due to variations in the thickness of the pressure sensitive adhesive and  
 251 imperfections (e.g. scratches) on the surface of the polymer.  
 252



253  
 254 **Figure 3: A comparison of the cavity output spectra for the glass and the Zeonor<sup>®</sup> flow**  
 255 **cells (where spectrometer integration time is 10 ms and a common normalisation**  
 256 **constant of 16383 was used for both glass and Zeonor<sup>®</sup>)**

257  
 258



259

260 **Figure 4: CEF of the flow cell made of Zeonor® vs. wavelength (where the inset depicts**  
 261 **the location of "C", "R" and "L" on the device and spectrometer integration time is 10**  
 262 **ms)**

263

264 A summary of other parameters of interest such as the relationship between absorbance and  
 265 concentration of potassium permanganate, CEF, LOD and minimum detectable absorption  
 266 coefficient of the glass and the Zeonor® flow cells at 572 nm is provided in Table 1.

267

Material	Fabrication method	Relation between absorbance and concentration	R <sup>2</sup>	CEF	LOD (μM)	Minimum detectable absorption coefficient (cm <sup>-1</sup> )
Glass	Commercially available	0.0099+3140.5c	0.999	115.3	1.0	2.6×10 <sup>-3</sup>
Zeonor®	Pressure sensitive adhesive	0.001+2458.5c	0.999	115.8	1.1	2.9×10 <sup>-3</sup>

268 **Table 1: Summary of the various parameters of interest for the flow cells at 572 nm**  
269 **(where  $\varepsilon = 2653 \text{ M}^{-1} \text{ cm}^{-1}$ ,  $c$  is the concentration of potassium permanganate in M and**  
270 **spectrometer integration time is 10 ms)**

271

272 Linear absorbance response was observed in the range from  $2.5 \times 10^{-5} \text{ M}$  to  $1 \times 10^{-3} \text{ M}$   
273 potassium permanganate for the Zeonor<sup>®</sup> device. The relationship between the absorbance  
274 and the concentration of potassium permanganate in the linear range for the device is given  
275 by  $A = 0.001 + 2458.5c$  with  $r^2 = 0.999$ . The CEF of the Zeonor<sup>®</sup> device at 572 nm is  $\sim 116$ . It is  
276 thought that the maximum achievable CEF is limited by the reflectivity of the mirrors used to  
277 perform the work. The effective optical path length is the product of the CEF and the physical  
278 dimension of a flow cell along the path of the light beam. Thus, the optical path length of the  
279 Zeonor<sup>®</sup> device can be increased from 80  $\mu\text{m}$  to 9.3 mm at the chosen conditions. The LOD  
280 of potassium permanganate was 1.1  $\mu\text{M}$  at 572 nm, which corresponds to a minimum  
281 detectable absorption coefficient of  $2.9 \times 10^{-3} \text{ cm}^{-1}$ . This is two orders of magnitude better than  
282 the typical LOD obtained via single pass absorbance spectroscopy in microfluidic flow cells  
283 [30]. Thus, BBCEAS is well suited to perform high sensitivity detection in the microfluidic  
284 flow cell made of Zeonor<sup>®</sup>.

285

286 A possible application of the Zeonor<sup>®</sup> device interfaced with BBCEAS is in multi-  
287 wavelength spectrometric measurements for simultaneous detection of, for example,  
288 Haemoglobin derivatives [31]. Another possible application could be in the sensitive  
289 detection of (bio) chemical species (e.g. proteins, iron, calcium and so on) in microfluidic  
290 flow cells via colorimetric assays.

291

#### 292 **4. Conclusions**

293 Absorbance is a widely applicable detection technique, but the sensitivity of absorbance  
294 spectroscopy in microfluidic devices is normally restricted by the short optical path length of  
295 the microchannels. One way of increasing the effective optical path length is by using  
296 broadband cavity enhanced absorption spectroscopy (BBCEAS) in which the device is placed  
297 inside a cavity comprising high reflectivity mirrors to achieve multiple passes through the  
298 sample. The suitability of BBCEAS as a detection technique has so far only been  
299 demonstrated for devices made of glass. This paper for the first time investigates the  
300 feasibility of BBCEAS as a detection technique for a microfluidic flow cell made of Zeonor<sup>®</sup>,  
301 which is important because the device is particularly well suited for single-use applications

302 such as clinical diagnostics. Zeonor<sup>®</sup> is cheaper, simpler to process and easier to dispose of  
303 than glass. In addition, Zeonor<sup>®</sup> devices can be mass produced using techniques such as  
304 injection moulding.

305

306 In this work, an optical cavity was formed from two mirrors, with reflectivity of  $99\pm 0.3\%$  in  
307 the wavelength range between 400 nm and 800 nm, placed 13 cm apart. Simultaneous  
308 measurements were made at all wavelengths in the absorption region, ranging from 480 nm  
309 to 600 nm, of potassium permanganate. The wavelength range studied was determined by the  
310 supercontinuum light source and the absorber (rather than the transmission characteristics of  
311 the polymer material) used. The CEF of the Zeonor<sup>®</sup> device constructed using the pressure  
312 sensitive adhesive bonding method was enhanced by two orders of magnitude. For example,  
313 the CEF of the Zeonor<sup>®</sup> device was 116 at 572 nm, which corresponds to a detection  
314 sensitivity of  $2.9\times 10^{-3}\text{ cm}^{-1}$  or 1.1  $\mu\text{M}$  potassium permanganate. In conclusion, BBCEAS is  
315 well suited as a detection technique for the microfluidic device made of Zeonor<sup>®</sup>.

316

317 Although this study was performed in the wavelength range between 480 nm and 600 nm, the  
318 set-up is universal provided that suitable light sources, mirrors and absorbing species are  
319 used. In case single-wavelength measurement is desirable, the instrumentation can be  
320 simplified by replacing, for example, the supercontinuum light source and the spectrometer  
321 by a laser and a charge coupled device respectively. The suitability of interfacing BBCEAS  
322 with microfluidic devices made of other polymers will be investigated in future. Future work  
323 will also concentrate on interfacing injection moulded Zeonor<sup>®</sup> devices with BBCEAS to  
324 determine bio(chemical) species.

325

### 326 **Acknowledgments**

327 The Zeonor<sup>®</sup> ZF14-188 film was kindly donated by Zeon Chemicals Europe Ltd. We would  
328 like to thank Simon R. T. Neil and Dr. Jeff Prest for useful discussions.

329

### 330 **References**

- 331 [1] J.C. Jokerst, J.M. Emory, C.S. Henry, *Analyst* 137 (2012) 24.  
332 [2] A.G. Crevillén, M. Hervás, M.A. López, M.C. González, A. Escarpa, *Talanta* 74  
333 (2007) 342.  
334 [3] D. Erickson, D. Li, *Anal. Chim. Acta* 507 (2004) 11.  
335 [4] M.A. Schwarz, P.C. Hauser, *Lab Chip* 1 (2001) 1.

- 336 [5] M. Albin, R. Weinberger, E. Sapp, S. Moring, *Anal. Chem.* 63 (1998) 417.
- 337 [6] O.J.A. Schueller, X.M. Zhao, G.M. Whitesides, S.P. Smith, M. Prentiss, *Adv. Mater.*  
338 11 (1999) 37.
- 339 [7] C. Gooijer, G.P. Hoorweg, T. de Beer, A. Bader, D.J. van Iperen, U.A.T. Brinkman,  
340 *J. Chromatogr. A* 824 (1998) 1.
- 341 [8] K. Fujiwara, J.B. Simeonsson, B.W. Smith, J.D. Winefordner, *Anal. Chem.* 60 (1988)  
342 1065.
- 343 [9] M.P. Duggan, T. McCreedy, J.W. Aylott, *Analyst* 128 (2003) 1336.
- 344 [10] A. Datta, I.Y. Eom, A. Dhar, P. Kuban, R. Manor, I. Ahmad, S. Gangopadhyay, T.  
345 Dallas, M. Holtz, H. Temkin, P.K. Dasgupta, *IEEE Sens. J.* 3 (2003) 788.
- 346 [11] N.J. Goddard, J. Hulme, C. Malins, K. Singh, P.R. Fielden, *Analyst* 127 (2002) 378.
- 347 [12] F. Prieto, L.M. Lechuga, A. Calle, A. Llobera, C. Dominguez, *J. Lightwave Technol.*  
348 19 (2001) 75.
- 349 [13] G. Pandraud, T.M. Koster, C. Gui, M. Dijkstra, A. van den Berg, P.V. Lambeck,  
350 *Sens. Actuators A* 85 (2000) 158.
- 351 [14] A. Prabhakar, S. Mukherji, *Lab Chip* 10 (2010) 748.
- 352 [15] A. Grazia, M. Riccardo, F.L. Ciaccheri, *Appl. Spectrosc.* 52 (1998) 546.
- 353 [16] S. McNab, N. Moll, Y.A. Vlasov, *Opt. Express* 11 (2003) 2927.
- 354 [17] A. Nitkowski, L. Chen, M. Lipson, *Opt. Express* 16 (2008) 11930.
- 355 [18] A. Nitkowski, A. Baeumner, M. Lipson, *Biomed. Opt. Express* 2 (2011) 271.
- 356 [19] M. Islam, L.N. Seetohul, Z. Ali, *App. Spectrosc.* 61 (2007) 649.
- 357 [20] S.R.T. Neil, C.M. Rushworth, C. Vallance, S.R. Mackenzie, *Lab Chip* 11 (2011)  
358 3953.
- 359 [21] H. Zhu, M. Holl, T. Ray, S. Bhushan, D.R. Meldrum, *J. Micromech. Microeng.* 19  
360 (2009) 065013.
- 361 [22] T. McCreedy, *TrAC Trends Anal. Chem.* 19 (2000) 396.
- 362 [23] C. Jönsson, M. Aronsson, G. Rundström, C. Pettersson, I. Medl-Hartvig, J. Bakker, E.  
363 Martinsson, B. Liedberg, B. MacCraith, O. Öhman, J. Melin, *Lab Chip* 8 (2008) 1191.
- 364 [24] P. Sabounchi, A.M. Morales, P. Pounce, L.P. Lee, B.A. Simmons, R.V. Davalos,  
365 *Biomed. Microdevices* 10 (2008) 661.
- 366 [25] P.S. Nunes, P.D. Ohlsson, O. Ordeig, J.P. Kutter, *Microfluid. Nanofluid.* 9 (2010)  
367 145.
- 368 [26] B. Kuswandi, Nuriman, J. Huskens, W. Verboom, *Anal. Chim. Acta* 601 (2007) 141.

- 369 [27] M. Mazurenka, A.J. Orr-Ewing, R. Peverall, G.A.D. Ritchie, *Annu. Rep. Prog. Chem.*  
370 *Sect. C* 101 (2005) 100.
- 371 [28] J.N. Miller, J.C. Miller, *Statistics and Chemometrics for Analytical Chemistry*,  
372 Harlow: Pearson Prentice Hall, Essex, 2010.
- 373 [29] M. Yamazaki, *J. Mol. Catal. A Chem* 213 (2004) 81.
- 374 [30] B. Kuswandi, Nuriman, J. Huskens, W. Verboom, *Anal. Chim. Acta* 601 (2007) 141.
- 375 [31] A. Zwart, A. Buursma, E.J. van Kampen, B. Oeseburg, P.H.W. van der Ploeg, W.G.  
376 Zijlstra, *J. Clin. Chem. Clin. Biochem.* 19 (1981) 457.